

Statistical Analysis of Bend Strength Data According to Different Evaluation Methods

M. Steen,^a S. Sinnema^b & J. Bressers^a

^aInstitute for Advanced Materials, Joint Research Centre, CEC, P.O. Box 2, 1755 ZG Petten, The Netherlands

^bHoogovens Ijmuiden, Research and Works Laboratories, Steelmaking Metallurgy and Refractories, P.O. Box 10 000, 1970 CA Ijmuiden, The Netherlands

(Received 18 February 1991; revised version received 9 September 1991; accepted 10 September 1991)

Abstract

The strength values obtained in four series of bend tests on two monolithic ceramic materials have been statistically evaluated. Statistical mapping procedures were used to check whether a Weibull distribution fits the strength data. Where this has been found to be the case, the value of the Weibull parameters determined according to different evaluation methods fall within each other's confidence interval. The values of the modulus m and of the characteristic strength σ_0 of the two-parameter distribution can differ significantly from the corresponding values in the three-parameter distribution.

Die Festigkeitswerte von zwei monolithischen Keramiken wurden durch Biegeversuche in vier Serien bestimmt und statistisch ausgewertet. Hierzu wurden verschiedene statistical mapping angewandt um zu klären, ob die Festigkeitsdaten einer Weibull-Verteilung folgen. Wo dies der Fall war, fielen die Weibull-Parameter, die nach den verschiedenen Auswertungsmethoden bestimmt wurden, in die jeweils gegenseitigen Konfidenzintervalle. Die Werte des Moduls m und der charakteristischen Festigkeit σ_0 der zweiparametrischen Verteilung können stark von den entsprechenden Werten der dreiparametrischen Verteilung abweichen.

On a traité statistiquement les valeurs de résistance mécanique obtenues au cours de quatre séries d'essais en flexion réalisés sur deux céramiques monolithiques. Statistical mapping de cartographie étaient mises en oeuvre afin d'estimer si une distribution de Weibull était adaptée aux valeurs de la résistance mécanique. Lorsque cela est le cas, les valeurs du paramètre de Weibull déterminées selon les différentes méthodes d'évaluation sont situées dans le même intervalle de confiance. Les valeurs du module m et de la résistance

mécanique caractéristique σ_0 de la distribution à deux paramètres peuvent différer très sensiblement des valeurs correspondantes de la distribution à trois paramètres.

1 Introduction

The strength of a ceramic material is a statistical quantity which is sensitive to the defect population within the material. Probabilistic design concepts are therefore more appropriate for ceramics than the conventional concepts used for metallic components. The statistical analysis methods used to represent the strength variability in ceramic materials are mostly based on the well-known Weibull distribution function. The purpose of this paper is to investigate the applicability of this distribution function to four series of bend strength data obtained on two monolithic ceramic materials and to assess the effect of different methods for determining the parameters of the distribution.

2 Theoretical Background

2.1 Weibull function

Failure of brittle materials is normally described according to the weakest link model. The most commonly used statistical distribution function to represent the failure strength is due to Weibull.¹ The failure probability P at a given applied stress σ according to this distribution is given by:

$$P = 1 - \exp \left[- \left\{ \frac{\sigma - \sigma_u}{\sigma_0} \right\}^m \right] \quad (1)$$

This equation represents the three-parameter Weibull function with the shape parameter m

(Weibull modulus), the scaling parameter σ_0 (characteristic stress) and the location parameter σ_u (threshold stress). In the majority of cases, for reasons of ease of evaluation and of conservatism, the value of σ_u is taken to be zero.² This results in the two-parameter Weibull equation:

$$P = 1 - \exp[-(\sigma/\sigma_0)^m] \quad (2)$$

It should be remembered here that the value of the scaling parameter σ_0 depends on the dimensions (e.g. the volume and/or external surface area) of the tested specimen or component.

2.2 Methods to determine the Weibull parameters

Various methods exist to determine the Weibull parameters m and σ_0 from a set of experimental data. They can be divided into two groups: methods that are based on fitting the data to the non-linear eqn (2), and methods which rely on a linearization of that equation.

2.2.1 Non-linear equation methods

Three different methods can be used to determine m and σ_0 from the non-linear eqn (2).

2.2.1.1 Method of moments.^{2,3} In this method, the moments of the experimental failure distribution are set equal to the moments of the theoretical Weibull distribution. This results in the following set of equations which can be solved for m and σ_0 :

$$\bar{x} = \sigma_0 \Gamma\left(1 + \frac{1}{m}\right) = \sigma_0 \left(\frac{1}{m}\right)! \quad (3)$$

$$s/\bar{x} = \frac{\left[\Gamma\left(1 + \frac{2}{m}\right) - \Gamma^2\left(1 + \frac{1}{m}\right)\right]^{1/2}}{\Gamma\left(\frac{1}{m}\right)} \quad (4)$$

where \bar{x} and s represent the mean value and the standard deviation of the experimental results respectively and Γ is the gamma function. In a wide range of m values eqn(4) can be approximated by:³

$$m = -0.621 + 1.2785\bar{x}/s \quad (5)$$

Consequently, using the experimental values of \bar{x} and s , eqns (5) and (3) can be used to determine m and σ_0 .

2.2.1.2 Maximum likelihood method.^{2,3} According to this method, estimates of the parameters m and σ_0 are obtained by solving the following set of

equations derived from maximizing the likelihood function:

$$\frac{n}{m} + \sum \ln \sigma - n \frac{\sum \sigma^m \ln \sigma}{\sum \sigma^m} = 0 \quad (6)$$

$$\sigma_0 = \left[\frac{1}{n} \sum \sigma^m\right]^{1/m} \quad (7)$$

where n represents the total number of results. This non-linear set of equations is solved through an iteration procedure (e.g. by using the Newton-Raphson method).

2.2.1.3 Direct non-linear least squares analysis.

This method is usually referred to in the literature as a possibility and involves complex, non-easily programmable computations.³ Its interest on the practical level is rather limited.

2.2.2 Methods based on the linearized form of eqn (2)

2.2.2.1 Conventional analysis. Taking double logarithms of eqn (2) results in:

$$\ln \ln \frac{1}{1-P} = m \ln \sigma - m \ln \sigma_0 \quad (8)$$

In order to apply linear regression to this equation (from which the values of m and σ_0 can be determined), numerical values must be assigned to the left-hand side, i.e. a choice has to be made for the experimental definition of the failure probability P . A number of different estimators for P have been put forward in the literature,^{2,4} the most common ones being:

$$P_i = \frac{i - 0.5}{n}$$

and

$$P'_i = \frac{i}{n+1}$$

where i represents the rank number and n is the total number of results. Among these estimators, the first one is favoured because it results in the smallest bias on the derived value of the Weibull modulus m (see next section).

2.2.2.2 Application of a weight function. Least-squares linear regression analysis on the linearized eqn (8) assumes that the values of $\ln \sigma$, and not of σ , are distributed normally around the 'true' straight line. Since this is not the case, a weight function should be used. The appropriate form of the weight function reads:^{3,5}

$$W_i = [(1 - P_i) \ln(1 - P_i)]^2 \quad (9)$$

This weight function must be applied to the sum of squares of the deviations of the data from the straight line fit. It is claimed³ that application of this weight function to the linearized eqn (8) results in very similar estimates for m and σ_0 as those obtained through a direct non-linear least-squares analysis on eqn (2).

2.3 Bias and coefficient of variation on the estimate of the Weibull modulus m

For small sample sizes ($n \leq 100$), all methods for the estimation of the parameter m result in biased estimations, i.e. the estimated value of m is not exactly equal to the value of the true population parameter. In order to determine the bias associated with the different estimation methods, Monte-Carlo simulations have been performed.²⁻⁵ With the exception of the method of moments, only a single value of the true m must be considered to obtain the bias and the coefficient of variation for all possible values of m .

Next to the occurrence of bias in small sample sizes, there also exists an effect of statistical variability. Indeed, strength testing involves taking a random sample from, in principle, an infinite amount of specimens. Because of the limited sample size (i.e. the number of specimens tested), it cannot be expected that the mother population will be described exactly. This means that for a particular estimation method each sample will have different m and σ_0 values which will differ from the true values. These sample values are distributed normally and can thus be characterized by an average value and a variation coefficient. For the methods where an estimator for the probability of failure is needed, the bias and the coefficient of variation obviously depend on the estimator used.

The values of bias and coefficient of variation for the Weibull modulus m are listed in the tables in Appendix 1. It is observed that the bias is markedly less when the estimator $P_i = (i - 0.5)/n$ is used instead of $P'_i = i/(n + 1)$. When the former estimator is used, there is no significant improvement by using a weight function. However, this does not imply that the two methods, i.e. using a weight function or not, are equivalent for this estimator, since the data in the table only reflect the statistical behaviour. Individual m values determined according to both methods can be significantly different. In view of the point raised in the previous section, the use of a weight function should be favoured.

On the basis of the criterion of minimum bias, the weight function method is preferred. However, since for a particular evaluation method, the value of the

bias is known from the tables in Appendix 1, the criterion of minimum coefficient of variation could equally well be used. In that case, the maximum likelihood method is to be favoured.

2.4 Statistical mapping

In the previous sections, attention has been focused on the Weibull distribution as the most commonly used 'weakest-link' descriptor for failure of brittle materials. It suffers, however, from the major drawback that it has no basis in the physics of the failure process. Consequently the question can be raised to what extent a purely empirical distribution can be used confidently to represent experimental strength data. The quality of this representation, i.e. the degree of fit, also significantly affects any extrapolation of the data outside the experimentally covered range of failure probabilities.

In order to assess the suitability of a theoretical distribution function for describing the experimental data, statistical mapping procedures can be used. The concept and procedures for applying statistical mapping are outlined in greater detail in Appendix 2. Only the main points are summarized here. In a statistical map two non-dimensional shape factors (β_1 , skewness and β_2 , kurtosis), calculated from the moments of the distribution, are used to trace the movement of theoretical distributions.⁶ In a (β_1, β_2) -plot the theoretical distribution functions with two *shape* parameters are represented by a bounded area, those characterized by one shape parameter (e.g. Weibull) are represented by continuous lines and those without shape parameter by a fixed point. The shape factors best suited for application to small sample sizes (as encountered in practice) are based on probability weighted moments. The non-dimensional shape factors τ_3 and τ_4 (corresponding to the experimental data set) are calculated from the moments in which the theoretical expectation and the random variable are replaced by the average value and the sample values, respectively (see Appendix 2). To select the distribution function for the experimental data, the empirical values τ_3 and τ_4 are plotted in the statistical map. The continuous line passing closest to the point (τ_3, τ_4) corresponds to the distribution with one shape parameter which best fits the experimental data.

3 Experimental Procedure

A sintered alumina and a TZP-Y-stabilized zirconia have been investigated in this study. The materials

Table 1. Experimental bend strength values

Material	Configuration	Number of specimens	Strength range (MPa)	Average (MPa)	Standard deviation (MPa)
Zirconia	$b = 4, h = 3$ mm	23	450–742	679	75
	$b = 3, h = 4$ mm	24	490–774	681	66
Alumina	$b = 4, h = 3$ mm	24	253–341	297	25
	$b = 3, h = 4$ mm	25	220–326	283	32

were delivered in the form of plates. Bend specimens were machined from these plates in the longitudinal direction on a flat grinding machine, followed by precision grinding. The bend specimens were neither polished, nor were the edges chamfered. The nominal dimensions are $3 \times 4 \times 52$ mm³. The dimensional variations were well within the allowable tolerances of ASTM C28.01, AFNOR B41-104 and DIN 51 110.

The bend tests were performed under four-point loading at room temperature using a non-articulating stainless steel bending fixture with outer and inner spans of 40 mm and 20 mm, respectively. The roller-bearings were free to rotate around their axis. Tests were performed at a constant outer fibre stress rate of 26 MPa s⁻¹ for alumina and 10 MPa s⁻¹ for zirconia. For both materials these figures correspond to a deflection rate of 0.5 mm min⁻¹ and an outer fibre strain rate of 6.8×10^{-5} s⁻¹.

For each material, two series of bend tests were performed. In the first series, the normal configuration (3 mm height of the specimen) was used, while for the second series the height h was replaced with the width b . For the calculation of the bend strength, average values for the height and width measured in the centre and on two equidistant locations were used. Prior to testing, the bend specimens were randomized. The experimental bend strength values are summarized in Table 1.

4 Discussion

4.1 Weibull parameters

The experimental bend strength data are analysed according to the different evaluation methods outlined. The resulting values of the Weibull modulus m and of the characteristic strength σ_0 are summarized in Table 2. Where an estimator is needed, $P_i = (i - 0.5)/n$ has been used.

The value of the Weibull modulus ranges from 9.34 to 15.34 and from 9.65 to 14.38 for zirconia and alumina, respectively. The spread in characteristic strength values is much smaller and ranges from 706 to 718 MPa and from 296 to 308 MPa for zirconia and alumina, respectively. There is no clear tendency for any of the evaluation methods to yield higher or lower m values than the others.

Figures 1 and 2 show the experimentally obtained rupture strengths in a 'conventional' Weibull plot (the estimator $P_i = (i - 0.5)/n$ has been used). For zirconia (Fig. 1), the $b = 4$ mm test series exhibits an upward curvature, while this is not apparent for the $b = 3$ mm series. Such an upward curvature cannot be explained by a non-zero value of the threshold stress σ_u and has been considered indicative of the occurrence of two flaw populations.⁷ The experimental data obtained on the alumina, however, show evidence of a downward curvature which can

Table 2. Values of the shape parameter m and scaling parameter σ_0 obtained according to different evaluation methods

	Material	Configuration	Evaluation method			
			Linear regression	Weight function	Method of moments	Maximum likelihood
m	ZrO ₂	$b = 4, h = 3$ mm	9.34	14.15	10.97	15.34
		$b = 3, h = 4$ mm	11.80	14.04	12.56	14.46
	Al ₂ O ₃	$b = 4, h = 3$ mm	14.10	11.34	14.38	12.55
		$b = 3, h = 4$ mm	10.51	9.65	10.78	11.26
σ_0 (MPa)	ZrO ₂	$b = 4, h = 3$ mm	717	718	711	706
		$b = 3, h = 4$ mm	711	712	710	708
	Al ₂ O ₃	$b = 4, h = 3$ mm	308	307	308	308
		$b = 3, h = 4$ mm	296	298	296	296

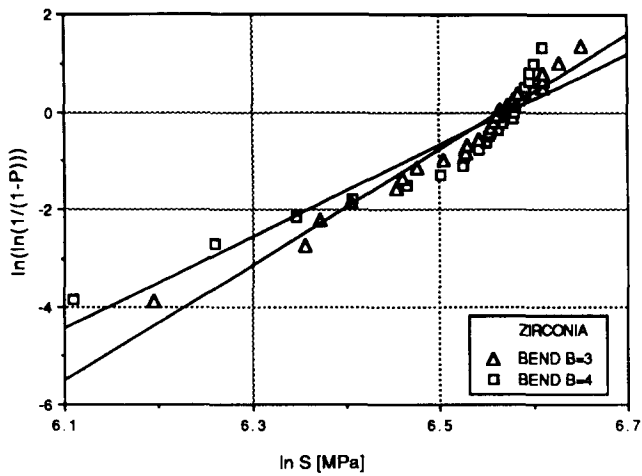


Fig. 1. Conventional Weibull plot of the bend data on zirconia.

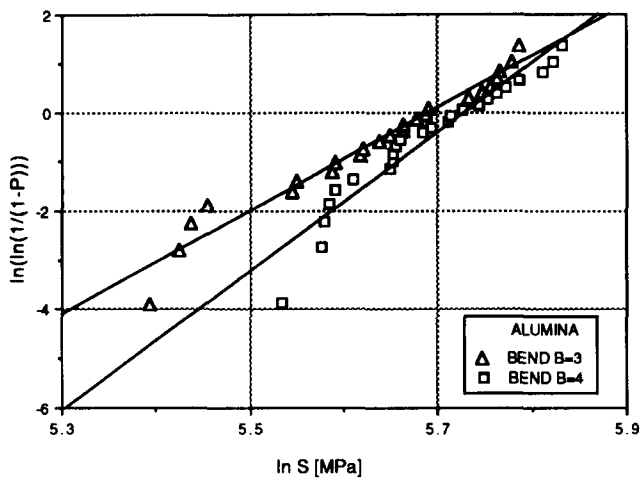


Fig. 2. Conventional Weibull plot of the bend data on alumina.

be explained by a threshold $\sigma_u > 0$ (Fig. 2). Figure 3 shows the cumulative failure probability plot for the $h = 4$ mm test series on alumina evaluated according to the different methods listed in Table 2. As can be observed, the results according to the different methods are rather similar. They all overestimate the failure probabilities both at low and high stresses.

When the respective values of the bias and the coefficient of variation (listed in Appendix 1) are taken into account, the ranges of m values listed in Table 3 are obtained (range = bias-corrected value \pm one standard deviation). Assuming that the m values determined according to any method are

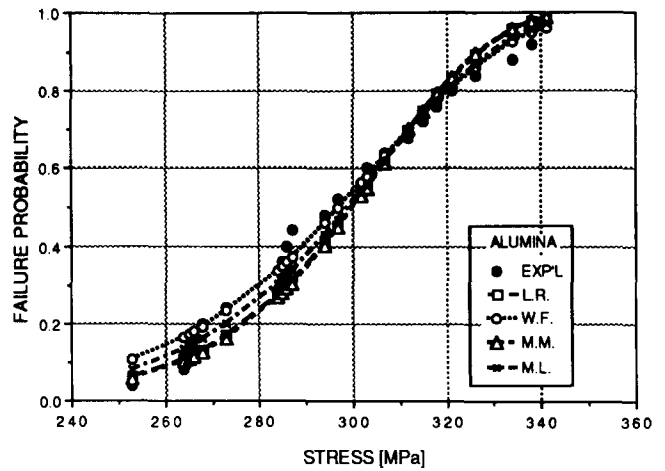


Fig. 3. Comparison between experimental and calculated cumulative failure probability plots for the bend test ($h = 4$ mm) on alumina.

normally distributed, this range corresponds to the 68% confidence interval.

Except for ZrO_2 tested in the $b = 4, h = 3$ mm configuration, the confidence intervals of m determined according to different evaluation methods overlap. This is also the case for the ranges corresponding to the two test configurations and determined according to a single evaluation method.

4.2 Statistical mapping

Figure 4 shows the representation of the Weibull distribution function in a statistical map, together with the working points (τ_3, τ_4) of the four test series. It can be observed that the $h = 4, h = 3$ mm bend test series on zirconia has a τ_3 value which lies outside the range of τ_3 values corresponding to the Weibull distribution. This implies that the latter is not an adequate representation of these experimental data. For the other test series acceptable (τ_3, τ_4) combinations are obtained, although they do not fall exactly on the curve representing the theoretical Weibull distribution.

Using the expressions for the first three probability weighted moments (see Appendix 2) of the Weibull distribution, which are used for the calculation of the value of τ_3 and τ_4 , a relationship between the parameters m and σ_u can be established.

Table 3. 68% Confidence intervals for the shape parameter m

Material	Configuration	Linear regression	Weight function	Method of moments	Maximum likelihood
ZrO_2	$b = 4, h = 3$ mm	7.24–11.27	11.31–17.27	8.35–12.46	11.65–17.05
	$b = 3, h = 4$ mm	9.20–14.20	11.29–17.08	9.61–14.25	11.08–16.06
Al_2O_3	$b = 4, h = 3$ mm	10.97–16.97	9.13–13.79	11.01–16.31	9.60–13.93
	$b = 3, h = 4$ mm	8.23–12.61	7.80–11.70	8.32–12.22	8.68–12.50

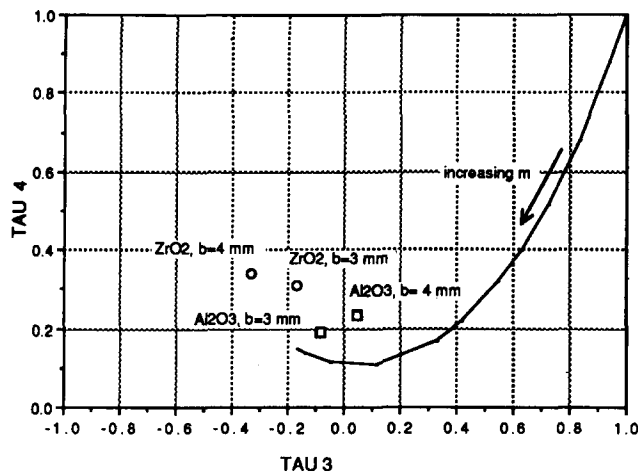


Fig. 4. Statistical map showing the curve corresponding to the Weibull distribution, together with the working points of the four test series.

Consequently the values of m and σ_0 corresponding to a zero threshold stress $\sigma_u = 0$ (i.e. two-parameter Weibull distribution) can be obtained. The results for the different test series are listed in Table 4. As can be observed, these values agree well with those listed in the previous table.

The expressions for the probability weighted moments in principle also allow the separate determination of the three Weibull parameters m , σ_0 and σ_u . A prerequisite is, however, that the experimental data can adequately be represented by a Weibull distribution. As mentioned before, and as shown in Fig. 4, this is not the case for one series of bend tests on ZrO_2 . Consequently, for this test series, the determination of the three parameters of the Weibull distribution is not possible. The results for the other series are summarized in Table 5.

Table 4. Values of the shape and scaling parameter determined through statistical mapping for a zero threshold stress

Material	Configuration	m for $\sigma_u = 0$	σ_0 (MPa) for $\sigma_u = 0$
ZrO_2	$b = 4, h = 3$ mm	9.74	715
	$b = 3, h = 4$ mm	10.47	715
Al_2O_3	$b = 4, h = 3$ mm	12.06	309
	$b = 3, h = 4$ mm	9.08	298

Table 5. Values of the Weibull parameters m , σ_0 and σ_u determined through statistical mapping

Material	Configuration	m	σ_0 (MPa)	σ_u (MPa)
ZrO_2	$b = 4, h = 3$ mm	—	—	—
	$b = 3, h = 4$ mm	90	5640	-4924
Al_2O_3	$b = 4, h = 3$ mm	2.2	74	232
	$b = 3, h = 4$ mm	7.0	237	61

The $b = 3$ mm test series on zirconia exhibits a negative threshold stress. This is physically unrealistic and reflects the purely empirical nature of the three-parameter Weibull distribution. For Al_2O_3 , positive threshold stress values are obtained, which agree with the graphical representation of Fig. 2. When a non-zero positive threshold stress σ_u is incorporated, the values of m and σ_0 strongly differ from those corresponding to a two-parameter distribution. Failure probabilities at low stresses calculated according to the latter are higher than those calculated from the former. For reasons of conservatism the two-parameter distribution is thus favoured.²

4.3 Analysis of the combined data sets per material

As mentioned before, the bend tests have been performed in two configurations on similar specimens by exchanging the width for the height. The most important effect of this is a change in the stress gradient through the specimen. To a smaller extent, it also affects the value of the effective surface in both configurations, while the effective volume remains the same for equal values of the Weibull modulus m . Even taking into account that different values of m are obtained for the two configurations (see Table 2), the differences in effective volume and effective surface are small. Consequently, the major effect, if any, of the difference in strength values obtained in the two test configurations, is attributed to the different stress gradients.

The ratios of the failure strengths $\sigma_{b=4}/\sigma_{b=3}$ corresponding to a 50% failure probability are 1.048 for Al_2O_3 and 0.999 for ZrO_2 , respectively. Both these values are close to 1, indicating that the stress gradient does not play an important rôle. Consequently, failure depends on the absolute value of the outer fibre stress, implying that surface flaws are the dominant failure initiation sites. On this basis, the data from both test series for each material can be treated as originating from a single population. The results of the analysis of the combined data are shown in Figs 5 and 6. As can be observed, they can be well represented by a two-parameter Weibull distribution. In particular, it can be seen that the combined ZrO_2 data do not exhibit a pronounced two-slope behaviour, which is indicative for the occurrence of more than one flaw population. For both materials, the modulus of the combined data falls between that of the two separate series.

This argumentation concerns the dependence of the failure strength on the stress gradient. However, the Weibull modulus m can also be affected by the

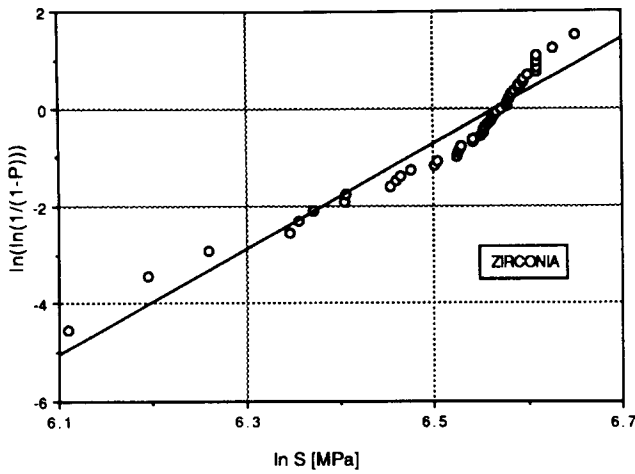


Fig. 5. Weibull plot of the combined bend data on zirconia.

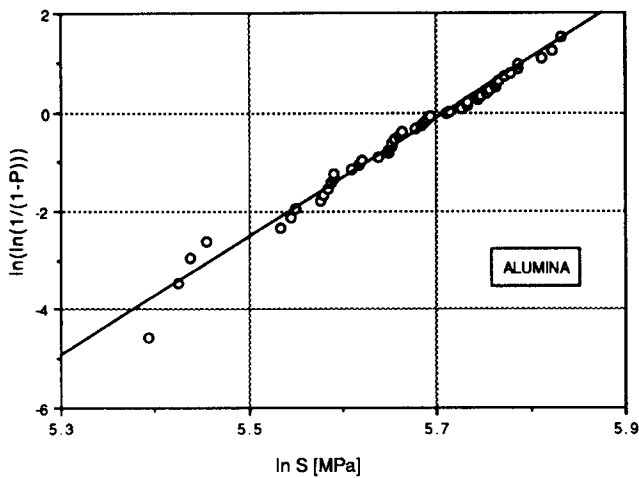


Fig. 6. Weibull plot of the combined bend data on alumina.

stress gradient. In the literature, a relationship between m and the stress gradient $d\sigma/dh$ is claimed in a number of cases.⁸ A tendency for the m value to decrease as the stress gradient increases is associated with the presence of two different flaw populations: surface flaws contribute more to fracture in the presence of a large stress gradient, while volume flaws are favoured in the case of a low stress gradient. As an operational definition of the stress gradient the following expression is used:

$$d\sigma/dh = \sigma_0/(h/2) = 2\sigma_0/h$$

Table 6 summarizes the values of m , σ_0 (conventional Weibull analysis) and $d\sigma/dh$.

The aforementioned tendency for m to decrease with an increase in $d\sigma/dh$ only occurs for ZrO_2 . This suggests that two flaw populations are present in the bend tests on ZrO_2 . Consequently the Weibull distribution is not the appropriate distribution to represent the experimental data. This is also

Table 6. Values of m , σ_0 and $d\sigma/dh$ for the different series of bend tests

Material	Configuration	m	σ_0 (MPa)	$d\sigma/dh$ (MPa/mm)
ZrO_2	$h = 4, h = 3$ mm	9.31	717	478
	$h = 3, h = 4$ mm	11.80	711	356
Al_2O_3	$h = 4, h = 3$ mm	14.10	308	205
	$h = 3, h = 4$ mm	10.51	296	148

confirmed by the fact that the τ_3 value corresponding to the data from both series does not fall within the range of validity for the Weibull distribution. For Al_2O_3 , an opposite trend occurs for m and $d\sigma/dh$ and no inferences can be made on the occurrence of one or more flaw populations.

4.4 Inferences on the occurrence of more than one flaw population

In the previous discussion, the possibility of the occurrence of more than one flaw population in the zirconia specimens has been touched upon a number of times. The most direct indications in this respect are that it is either impossible to determine the Weibull parameters ($h = 4$ mm specimens) or that awkward negative values for σ_u ($h = 3$ mm specimens) are obtained when the data are evaluated using statistical mapping procedures (see Table 5). Fractographic evidence to support the occurrence of a bimodal flaw population in the zirconia bend specimens is presented in a companion paper,⁹ where the flaw populations in bend and uniaxial tensile specimens are characterized. This finding corroborates the deductions made here on the occurrence of more than one flaw population through application of statistical mapping.

5 Conclusions

Different statistical evaluation methods have been applied to four series of bend tests on two materials. Statistical mapping has shown that the failure stresses of three series can be adequately represented by a Weibull distribution, while this is not possible for one series.

Determination of the parameters m and σ_0 of the two-parameter Weibull function according to different methods yields values of the parameters which fall within each other's confidence interval. This is not the case for the test series that cannot be adequately represented by a Weibull distribution function. For this test series it is deemed that two flaw populations occur simultaneously, thereby

invalidating the basic premise of the Weibull distribution, viz. that a single flaw population dominates failure over the full investigated stress range. Additional support is given by the inverse dependence of the modulus m on the stress gradient that is found for this test series.

Application of the statistical mapping method allows an easy numerical determination of the parameters of the three-parameter Weibull distribution in the case where the experimental data can be fitted by this distribution. The resulting values, specifically that of the modulus m , can be very different from those of a two-parameter distribution. Furthermore, the value of m is observed to inversely depend on the value of the threshold stress σ_u . Negative values of σ_u , which are physically unrealistic, are indicative of the occurrence of more than one flaw population.

Acknowledgements

The authors thank Hoogovens Ijmuiden for financial support and for providing the test specimens. They are also grateful to Mr J.-N. Adami, Mr G.

Bracke and Mr G. von Birgelen for their experimental assistance.

References

1. Weibull, W., A statistical distribution function of wide applicability. *J. Appl. Mech.*, **18** (1951) 293–7.
2. Trustrum, K. & De S. Jayatilaka, A., On estimating the Weibull modulus for a brittle material. *J. Mat. Sci.*, **14** (1979) 1080–4.
3. Bergman, B., How to estimate Weibull parameters. *Brit. Ceram. Proc.*, **39** (1987) 175–85.
4. Bergman, B., On the estimation of the Weibull modulus. *J. Mat. Sci. Lett.*, **3** (1984) 689–92.
5. Bergman, B., Estimation of Weibull parameters using a weight function. *J. Mat. Sci. Lett.*, **5** (1986) 611–14.
6. Snedden, J. & Sinclair, C., Statistical mapping and analysis of engineering ceramics data. In *Mechanics of Creep Brittle Materials*, ed. A. F. Cocks & A. R. Ponter. Elsevier Applied Science, London, 1989, pp. 99–116.
7. Johnson, C., Fracture statistics of multiple flaw distributions. In *Fracture Mechanics of Ceramics*, Volume 5, ed. R. Bradt, A. Evans, D. Hasselman & F. Lange, Plenum Press, New York, London, 1977, pp. 365–86.
8. Ikeda, K., Igaki, H. & Kuroda, T., Fracture strength of alumina under uniaxial and triaxial stress states, *Am. Ceram. Soc. Bull.*, **65** (1986) 683–8.
9. Steen, M., Sinnema, S. & Bressers, J., Study of the size effect on strength in bend and tensile tests on Al_2O_3 and ZrO_2 . *J. Eur. Ceram. Soc.*, submitted.

Appendix 1: Bias and Coefficient of Variation (in parentheses) for the Weibull Modulus m Determined from Monte-Carlo Simulations²⁻⁵

Table A1.1. Methods based on non-linearized equation

n	Method of moments			Maximum likelihood
	$m = 5$	$m = 10$	$m = 25$	
10	1.098 (0.32)	1.132 (0.32)	1.159 (0.33)	1.165 (0.34)
20	1.044 (0.20)	1.063 (0.21)	1.076 (0.22)	1.078 (0.20)
30	1.028 (0.16)	1.037 (0.17)	1.049 (0.18)	1.048 (0.16)
40	1.019 (0.14)	1.032 (0.14)	1.038 (0.16)	1.035 (0.13)
50	1.015 (0.12)	1.026 (0.13)	1.033 (0.14)	1.025 (0.12)

Table A1.2. Methods based on linearized equation

n	Least squares		Weight function	
	$P_i = \frac{i}{n+1}$	$P_i = \frac{i-0.5}{n}$	$P_i = \frac{i}{n+1}$	$P_i = \frac{i-0.5}{n}$
10	0.869 (0.33)	1.062 (0.33)	0.865 (0.31)	1.015 (0.33)
20	0.890 (0.24)	1.011 (0.23)	0.917 (0.20)	0.990 (0.22)
30	0.908 (0.19)	1.006 (0.19)	0.937 (0.17)	0.990 (0.18)
40	0.918 (0.17)	1.002 (0.17)	0.955 (0.15)	0.992 (0.15)
50	0.924 (0.14)	0.998 (0.14)	0.963 (0.14)	0.995 (0.14)
100	0.952 (0.10)	0.997 (0.10)	0.982 (0.10)	0.998 (0.10)

Appendix 2: Statistical Mapping⁶

In a statistical map, two non-dimensional shape factors, β_1 and β_2 , are used to trace the movement of theoretical distributions. The shape factors are based upon the central moments, i.e. moments about the mean μ , of the distribution according to

$$\beta_1 = \mu_3^2 / \mu_2^3 \text{ (skewness)}$$

and

$$\beta_2 = \mu_4 / \mu_2^2 \text{ (kurtosis)}$$

where μ_k represents the k th central moment

$$\mu_k = \sum_i (x_i - \mu)^k p(x_i)$$

for a discrete variable x with a probability density function $p(x_i)$.

The evaluation of the theoretical values of β_1 and β_2 can be quite difficult for some distributions. Fortunately, the evaluation of the empirical values of $\bar{\beta}_1$ and $\bar{\beta}_2$ from experimental data involves only elementary arithmetic.

The basic concept of using a statistical map as a guide to the most appropriate distribution simply involves plotting the values of $\bar{\beta}_1$ and $\bar{\beta}_2$ on the theoretical map. However, the standardized skewness β_1 is an even function and hence cannot represent negative skewness. In order to do so, β_1 is replaced by $\alpha_3 = \mu_3 / \mu_2^{3/2} = \beta_1^{1/2}$.

In practice, small sample sizes are encountered in the majority of cases. Under these conditions, the use of probability weighted moments is preferred over using the central moments.⁶ The first four probability weighted moments of a theoretical distribution function are given by

$$A_i = E[X(1 - F(X))^i] \quad i = 0, 1, 2, 3$$

where E is the theoretical expectation, X the random variable and $F(X)$ the theoretical cumulative distribution function. To obtain small sample equivalents, the expectation E is replaced by the average and X by the sample values X_i . For $F(X)$ the estimator $P_i = (i - 0.35)/n$ is used, where i represents the rank and n the total number of data. In constructing the statistical map, linear combinations of the empirical equivalents of the A_i moments are used:⁶

$$\begin{aligned} L_1 &= A_0 \\ L_2 &= A_0 - 2A_1 \\ L_3 &= A_0 - 6A_1 + 6A_2 \\ L_4 &= A_0 - 12A_1 + 30A_2 - 20A_3 \end{aligned}$$

from which the values of τ_3 (skewness) and τ_4 (kurtosis) can be finally calculated as

$$\tau_3 = L_3 / L_2 \quad \tau_4 = L_4 / L_2$$

To select the most appropriate distribution describing the experimental data, the empirical values of τ_3 and τ_4 are plotted in a theoretical (τ_3, τ_4) diagram (i.e. the statistical map). The continuous line, representing a theoretical distribution function with one shape parameter, passing closest to the experimental (τ_3, τ_4) point corresponds to the distribution which best fits the experimental data.